

Heat flux modulation in domino dynamo model

Maxim Reshetnyak*

Institute of the Physics of the Earth, Russian Academy of Sciences, Moscow, Russia

Pavel Hejda

Institute of Geophysics, Czech Academy of Sciences, Prague, Czech Republic

(Dated: August 27, 2021)

Using the domino dynamo model, we show how variations of the heat flux at the core-mantle boundary change the frequency of geomagnetic field reversals. In fact, we are able to demonstrate the effect known from the modern 3D planetary dynamo models using an ensemble of interacting spins, which obey equations of the Langevin type with a random force. We also consider applications to the giant planets and offer explanations of some specific episodes of the geomagnetic field in the past.

PACS numbers: 91.25.Mf, 52.30.-q

Generation of the planetary magnetic fields is a subject of the dynamo theory, which describes successive transformations of thermal and gravitational energy, concerning compositional convection, to energy of kinetic motions of the conductive liquid and then to the energy of the magnetic field [1]. Modern dynamo models include partial differential equations of thermal and compositional convection as well as the induction equation for the magnetic field, which some reasons should be three dimensional [2]. Although, due to the finite conductivity of the Earth's mantle, observations of the geomagnetic field at the Earth's surface are bounded by the first thirteen harmonics in the spherical function decomposition, one needs small-scale resolution down to $\sim 10^{-8} L$, to provide the necessary force balance in the core. Here $L \approx 2.2 \cdot 10^6 \text{m}$ is the scale of the liquid core. This difficulty is caused by the huge hydrodynamic Reynolds number $Re \sim 10^9$ as well as by the strong anisotropy of convection [3] due to the geostrophic state in the core [4]. Convection in the core is cyclonic. The cyclones and anticyclones are aligned with the axis of rotation, and their scale is much smaller than their length. As a result one needs very efficient computer resources to produce regimes in the desired asymptotic limit required for geodynamo simulations with grids 128^3 and more, which is a challenge even for modern supercomputers.

In spite of these technical problems, 3D dynamo models successfully mimic various features of the modern and ancient magnetic field including the reversals [5]. One of the important results of the dynamo theory is that the frequency of the reversals depends on the spatial distribution of the heat flux at the outer boundary of the liquid core [6]. In particular, the authors have shown that the increase of the heat flux along the axis of rotation leads to increase of the axial symmetry of the whole system and stops reversals. In a sense, the thermal trap of

reversals occurs. On the contrary, the decrease of the thermal flux at high latitudes leads to the chaotic behaviour of the magnetic dipole accompanied by frequent reversals, which is closely connected with the upsetting of the geostrophic balance and predominance of the radial (in an incompressible medium in which the parameters depend only on the radius) Archimedean forces. It looks attractive to obtain this result using toy dynamo models (such as the Rikitake and Lorentz models), which can provide extensive statistics and obviousness of the results, and simulate practically instantly, using just home PC, the number of reversals and excursions of the same order as known from paleomagnetism. The random force, which imitates the small-scale unresolved fluctuations, was included in some of these models [7].

For this reason we have selected the domino dynamo model [8, 9], which is an extension of the Ising-Heisenberg XY-models of interacting magnetic spins, for more details of the history of the problem and classification refer to [10].

The main idea of the domino model is to consider a system of N interacting spins \mathbf{S}_i , $i = 1 \dots N$, in media rotating with angular velocity $\boldsymbol{\Omega} = (0, 1)$. The spins are located over a ring, are of unit length and can vary angle θ from the axis of rotation on time t , so that $\mathbf{S}_i = (\sin \theta_i, \cos \theta_i)$. Each spin \mathbf{S}_i is forced by a random force, effective friction, as well as by the closest neighbouring spins \mathbf{S}_{i-1} and \mathbf{S}_{i+1} .

Following [8], we introduce kinetic K and potential U energies of the system:

$$\begin{aligned} K(t) &= \frac{1}{2} \sum_{i=1}^N \dot{\theta}_i^2, \\ U(t) &= \gamma \sum_{i=1}^N (\boldsymbol{\Omega} \cdot \mathbf{S}_i)^2 + \lambda \sum_{n=1}^N (\mathbf{S}_i \cdot \mathbf{S}_{i+1}). \end{aligned} \quad (1)$$

The Lagrangian of the system then takes the form $\mathcal{L} = K - U$. Making the transition to the Lagrange equations, adding friction proportional to $\dot{\theta}$ and the random force

*Electronic address: m.reshetnyak@gmail.com

χ ,

$$\frac{\partial}{\partial t} \frac{\partial \mathcal{L}}{\partial \dot{\theta}} = \frac{\partial \mathcal{L}}{\partial \theta} - \kappa \dot{\theta} + \frac{\epsilon \chi}{\sqrt{\tau}}, \quad (2)$$

leads to the system of Langevin-type equations [8]:

$$\begin{aligned} \ddot{\theta}_i - 2\gamma \cos \theta_i \sin \theta_i + \lambda \left[\cos \theta_i \left(\sin \theta_{i-1} + \sin \theta_{i+1} \right) - \right. \\ \left. \sin \theta_i \left(\cos \theta_{i-1} + \cos \theta_{i+1} \right) \right] + \kappa \dot{\theta}_i + \frac{\epsilon \chi_i}{\sqrt{\tau}} = 0, \\ \theta_0 = \theta_N, \theta_{N+1} = \theta_1, i = 1 \dots N, \end{aligned} \quad (3)$$

where γ , λ , κ , ϵ , τ are constants. The measure of synchronization of the spins along the axis of rotation

$$M(t) = \frac{1}{N} \sum_{i=1}^N \cos \theta_i(t) \quad (4)$$

will be considered to be the total axial magnetic moment.

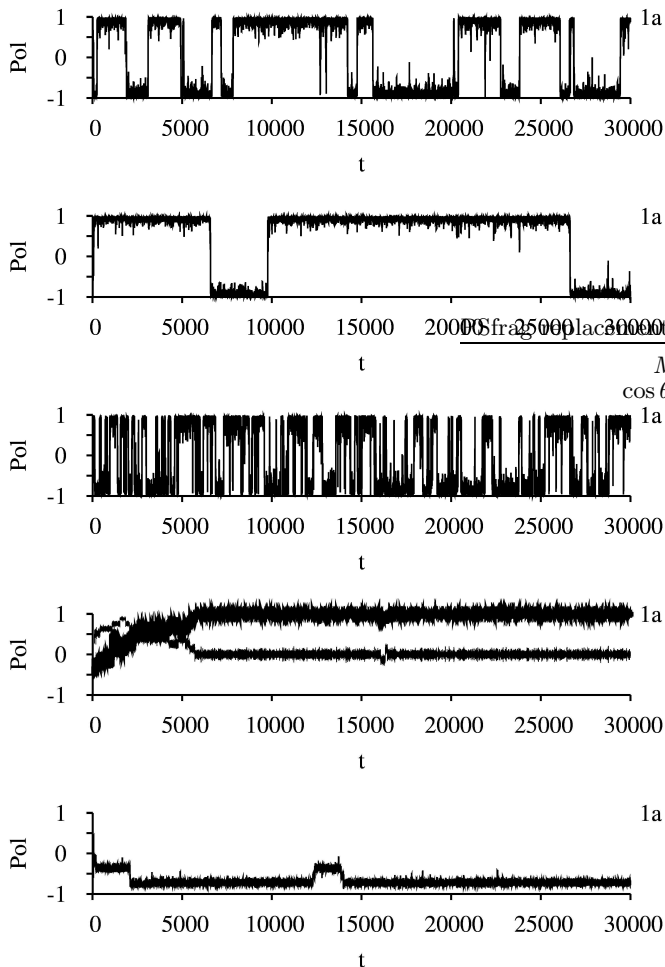


FIG. 1: Evolution in time of M : (a) for the purely magnetic system ($C_\psi = 0$), (b) $C_\psi = 0.5$, (c) $C_\psi = -0.5$ for $\psi = -\cos^2 \theta$, (d) $C_\psi = 10$, (e) $C_\psi = -9$ for $\psi = -\cos^2 2\theta$. At (d) the thick line corresponds to M and the thin line to M_e .

Integrating (3) in time for small N one can arrive at quite diverse dynamics of M , very close (for some special

choice of parameters) to paleomagnetic observations [11], including the periods of the random and frequent reversals. It was shown in [8] that large fluctuation of a single spin can be successively transferred to the neighbouring spins, which fluctuate until all spins reverse their polarity. This dynamo effect was an inspiration for the name "domino mode".

In all simulations we have used, similarly to [8], values of parameters $\gamma = -1$, $\lambda = -2$, $\kappa = 0.1$, $\epsilon = 0.65$, $\tau = 10^{-2}$, $N = 8$, with random normal χ_i , with zero mean values and unit dispersions, so that χ_i was updated at every time step equal to τ . As follows from [8] the evolution of M depends slightly on the form of the random forcing χ and the remaining parameters can be easily selected in such a way as to provide similarity with observations. The typical behaviour of the axial dipole is

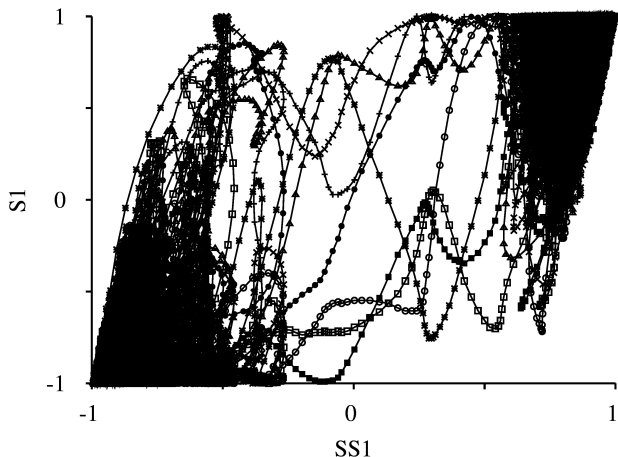


FIG. 2: Plots of $\cos \theta_i$ with $i = 1 \dots N$, versus M for reversal in Fig. 1a during the time interval $t = 10^3 - 3 \cdot 10^3$.

presented in Fig. 1a, where we observe several reversals at irregular time intervals. This process is accompanied by a short drop of M to nearly zero and followed by rapid recover, which in geomagnetism is referred to as excursions of the magnetic field. One can find a thorough analysis of this system in [8]; here we only emphasize one important in geomagnetism point. Up to now observations do not clearly indicate, if the geomagnetic dipole just rotates during the reversal without decreasing the amplitude, or if it decreases and then recovers with the opposite sign. To check these scenarios we present the evolution of the individual spins during the reversal, see Fig. 2. There are quite large deviations of the individual spins from the mean value M at the moment of reversal ($M = 0$). This means that the decrease of M is caused by the desynchronization of the spins rather than by the coherent rotation of the spins. Note that the typical time of the reversal is much larger than the time step. The points on the lines correspond to every 10^{th} time step in the simulations. The other point is that the minimal time $\sim N \tau / 2$ of propagation of the disturbance from spin S_i through half the circle is also smaller than the typical reversal time. This scenario is also supported by the 3D

simulations, where the spots of the magnetic field with opposite polarities co-exist at the core-mantle boundary during the reversals.

We now extend the concept of the spin from the purely magnetic system to the whole cyclone system, including its hydrodynamics, and we introduce correction Ψ to potential energy U (1), which takes into account the heterogeneity of the thermal flux. For the purely magnetic problem, it corresponds to the electromagnetic interaction of the cyclone with the conducting mantle, the D'' layer. The new effective force $F_i = -\frac{\partial \Psi_i}{\partial \theta_i}$, whose influence on the behaviour of $M(t)$ will be considered in the rest of the paper, then appears in the right-hand side of (3).

Let $\Psi(t, \theta) = C_\psi \psi(t, \theta)$, where C_ψ is a constant, and the spatial distribution of the potential is given by $\psi = -\cos^2 \theta$. Then, $C_\psi > 0$ corresponds to the stable state in the polar regions, $\theta = 0, \pi$, and the appearing force $F = -\sin 2\theta$, acting on the cyclones, is directed towards the poles. This regime corresponds to the increase of the thermal flux near the poles that causes the stretching of the cyclone along the axis of rotation. In Fig.1 we demonstrate the effective influence of F on M .

The increase of the thermal flux along the axis of rotation leads to the partial suppression of the reversals of the field, Fig.1b. Note that, for the chosen potential barrier ψ , the dependence of F is equal to the γ -term in (3): the increase of the thermal flux at the poles leads to the effective increase of rotation and amplification of geostrophy, caused by the rapid daily rotation of the planet. Our results are in agreement with the 3D simulations, see Fig.1d in [6]. The further increase of C_ψ ($C_\psi = 2$) leads to the total stop of the reversals. It is more interesting that, using even larger $C_\psi > 10$, one arrive at regimes with a nearly constant in time $|M| \leq 1$ defined by the initial distribution of \mathbf{S}_i . In other words, the super flux at the poles can fix the spins which are still not coherent. There is some evidence [12, 13] that the geomagnetic dipole in the past could have migrated from the usual position near the geographic poles to some stable state in the middle latitudes. Within the framework of our model, we can explain this phenomenon by the thermal super flux at the poles. Later we will discuss some other scenarios which yield similar results.

For negative C_ψ , when the geostrophy breaks due to the relative intensification of convection in the equatorial plane, we get the opposite result, see Fig.1c: the regime of the frequent reversals observed in Fig.1c in [6]. In this case force F is directed from the poles and the equilibrium point at the poles becomes unstable. The new

minimum of the potential energy at the equator leads to the appearance of a new attractor, so that for $C_\psi = -5$ the axial dipole fluctuates with zero mean value and maximal amplitude $M \sim 0.4$. This state corresponds to the equatorial dipole

$$M_e(t) = \frac{1}{N} \sum_{i=1}^N \sin \theta_i(t), \quad (5)$$

so that $|M_e| \sim 1$ and does not undergo reversal. Similar behaviour of the magnetic dipole is observed on Neptune and Uranus; for more details see, e.g. [14].

Now we consider $\psi = -\cos^2 2\theta$ for which the corresponding force $F = -2\sin 4\theta$ changes sign in each hemisphere, see the example with the second-order zonal spherical harmonic $\sim P_2^0$, where P_l^m is associated Legendre polynomials, in Fig.1e in [6].

For $C_\psi > 0$, the potential barrier is in the middle latitudes, which prohibits the reversals as observed in Fig.1e in [6]. In one of our runs only one reversal was observed at $C_\psi = 2$. The other important point is the existence of the stable point at the equator, where $M = 0$. We could then assume a regime with two attractors: near the poles and at the equator. This regime is really observed in Fig.1d. The inverse transition was not observed. Inspection of the state with small M at the beginning of the run leads to a quite large estimate of the equatorial dipole amplitude M_e , see Fig.1d. Thus, in principle, this regime can also be related to the giant planets' dynamo as.

The last example corresponds to the case when $C_\psi < 0$. Here in addition to the attractors at the poles (related to rotation Ω), two new attractors appear at middle latitudes. The variation of C_ψ , leads to regimes $C_\psi = -1$ with frequent reversals, observed in Fig.1f in [6]. Moreover, we can get regimes, see Fig.1e, when the magnetic pole stays at high latitudes, however, $|M| \neq 1$ (the partial synchronization of the spins). There are some jumps to the unstable state $M = 0$ with the dipole at the equator. Note that the decrease of the spatial scale of ψ leads to the increase of its amplitude C_ψ .

Obviously, as the interaction between the cyclones is certainly more complex [15] than in (1) and the mechanism of magnetic field generation in cyclonic turbulence is outside the scope of the domino model, our results should be used with caution. However, it is remarkable that even such a simple model provides quite a wide range of effects, known from very sophisticated models and observations. This, of course, does not exclude other explanations and scenarios of the considered phenomena.

[1] G. Rudiger, R. Hollerbach. *The Magnetic Universe: Geophysical and Astrophysical Dynamo Theory*. 2004. Weinheim.
 [2] C. A. Jones, *Annu. Rev. Fluid Mech.* **43**, 583 (2011)

[3] P. Hejda, M. Reshetnyak. Effects of anisotropy in the geostrophic turbulence. *Phys. Earth Planet. Int.* 2009. 177, 152-160.
 [4] Pedlosky J 1987 *Geophysical Fluid Dynamics* (NY,

Springer-Verlag)

- [5] U. R. Christensen, *J. Fluid. Mech.* **470**, 115 (2002)
- [6] G. A. Glatzmaier, R. S. Coe, L. Hongre, P. H. Roberts, *Nature*. **401**, 885 (1999)
- [7] P. Hoyng, *Astron. Astrophys.* **272**, 321 (1993)
- [8] N. Mori, D. Schmitt, A. Ferriz-Mas, J. Wicht, H. Mouri, A. Nakamichi, M. Morikawa. A domino model for geomagnetic field reversals. (2011). arXiv:1110.5062v1.
- [9] A. Nakamichi, H. Mouri, D. Schmitt, A. Ferriz-Mas, J. Wicht and M. Morikawa, Submitted to *Mon. Not. R. Astron. Soc.* (2012). arXiv:1104.5093v1.
- [10] H. E. Stanley, *Introduction to phase transitions and critical phenomena*. 1987. Oxford.
- [11] J. A. Jacobs, *Reversals of the Earth's Magnetic Field*. 1994. Cambridge.
- [12] A. V. Shatsillo, A. N. Didenko and V. E. Pavlov. Two competing Paleomagnetic directions in the Late Vendian: New data for the SW Region of the Siberian Platform, *Russ. J. Earth Sci.* **7**, 4 ES4002 (2005)
- [13] A. Abrajevitch, Rob Van der Voo. Incompatible Ediacaran paleomagnetic directions suggest an equatorial geomagnetic dipole hypothesis. *Earth and Planetary Science Letters*. **293** 164 (2010)
- [14] I. Cupal, P. Hejda, M. Reshetnyak, *Planet. Space Sci.* **50** 1117 (2002)
- [15] A. Kageyama and T. Sato, *Phys. Rev.* **E5**, 4, 4617 (1997)